

Magnetostatic Analysis of a Brushless DC Motor Using a Two-Dimensional Partial Differential Equation Solver

A. KOSTARIDIS, C. SORAS, V. MAKIOS

Laboratory of Electromagnetics, Department of Electrical and Computer Engineering, University of Patras, Greece

Received 8 January 2000; accepted 2 January 2001

ABSTRACT: A finite element, magnetostatic analysis, of a brushless direct current motor containing non-linear materials and permanent magnets is presented. The analysis is performed with PDEase™, a low cost, two-dimensional partial differential equation solver. The descriptor file is remarkably short and easy to understand, enabling students to focus on the application and not on the finite element method. ©2001 John Wiley & Sons, Inc. *Comput Appl Eng Educ* 9: 93–100, 2001

Keywords: brushless motor modeling; finite element method; permanent magnets; non-linear materials

INTRODUCTION

Electrical engineering students are taught the fundamental equations of electromagnetic field theory early in their academic curriculum, but these equations can be solved only for those problems which have analytical solution. Nowadays, with the widespread availability of personal computers, it is possible to solve field equations for the rest of the problems via a numerical method. Field simulations help engineering students to understand the interrelation among field quantities, sources and materials in a problem, and to vastly improve their visualization.

Among the various numerical methods for solving field equations, the finite element method (FEM) has

been known for several decades and applied to almost any kind of problem at both low and high frequencies. In order to exploit its powerful capabilities, students can either write their own code or modify an existing one or use a software package. The first two options are not practical for undergraduate students because they require knowledge beyond their level and considerable amount of time. On the other hand most software packages seem like black boxes since there is no access to the underlying field equations. The pedagogical gap between the source code and software package options can be smoothed with the aid of PDEase, a scalar finite element based solver of partial differential equations [1].

Any student who is familiar with the differential form of classic field theory can write a short problem descriptor file, specifying the mathematical model and the proper boundary conditions. The descriptor file is text based with a format very close to usual

Correspondence to V. Makios (v.makios@ee.upatras.gr).
© 2001 John Wiley & Sons, Inc.

mathematical notation. In addition, this format allows a problem to be parameterized in terms of variables, enabling thus quick trade-off studies by varying a single parameter. The descriptor file is solved automatically and the results appear in the form of plots as requested. PDEase has the capability of automatic mesh generation and mesh refinement which helps the user to focus on the application and not on the finite element method.

This paper demonstrates the use of PDEase in the analysis of a brushless DC motor. This is a magnetic field problem with non-linear materials and permanent magnets. The difficult task of entering the complicated geometry of this sample problem is greatly simplified through the use of a geometric modeler. The descriptor file for this problem is remarkably short and easy to understand from a student with no prior magnetic simulation or motor experience.

MAGNETOSTATIC FORMULATION

For static or slowly varying in time (quasi-static) magnetic fields, the field intensity (\underline{H}) and flux density (\underline{B}) must obey:

$$\nabla \times \underline{H} = \underline{J} \quad (1)$$

$$\nabla \cdot \underline{B} = 0 \quad (2)$$

subject to a constitutive relationship between \underline{B} and \underline{H} for each material. For non-magnetic and soft magnetic materials this relationship is:

$$\underline{B} = \mu \underline{H} \quad (3)$$

while for hard magnetic materials (permanent magnets):

$$\underline{B} = \mu(\underline{H} + \underline{H}_c) \quad (4)$$

where \underline{H}_c is the coercive field intensity of the permanent magnet [2]. For isotropic materials the magnetic permeability μ is:

$$\mu = \mu_0 \cdot \mu_r \quad (5)$$

where μ_r is its relative permeability and $\mu_0 = 4\pi \times 10^{-7}$ H/m. If a material is non-linear μ is a function of \underline{B} otherwise it is a constant.

In this paper the fields that satisfy the above equations will be calculated via the magnetic vector potential \underline{A} , defined by the equation:

$$\underline{B} = \nabla \times \underline{A} \quad (6)$$

which always satisfies (2). For every point of a computational domain except those inside permanent magnets, the combination of (1), (3), and (6) implies:

$$\nabla \times \left(\frac{1}{\mu} \nabla \times \underline{A} \right) = \underline{J} \quad (7)$$

whereas for points inside permanent magnets the corresponding equation resulting from (1), (4), and (6) is:

$$\nabla \times \left(\frac{1}{\mu} \nabla \times \underline{A} - \underline{H}_c \right) = \underline{J} \quad (8)$$

Equation (8) is valid for every point in a computational domain and for all materials since it incorporates (7) for space regions outside permanent magnets by simply setting there $\underline{H}_c = 0$. Thus, the advantage of using the vector potential formulation is that equations (1)–(4) which form the mathematical model of the problem have been combined into a single equation. In the general three-dimensional case, \underline{J} and \underline{A} are vectors with three components each. In the two-dimensional case, however, four of these components are zero, leaving only the components in the “out of the page” direction, i.e., $\underline{J} = J(x,y)\underline{a}_z$ and $\underline{A} = A(x,y)\underline{a}_z$. If \underline{A} is found, \underline{B} and \underline{H} can then be deduced from (6) and (3) or (4) respectively.

TORQUE CALCULATION USING THE MAXWELL STRESS METHOD

The most important parameter to calculate is often the magnetically produced torque for a given rotor position and current excitation. For the torque calculation different methods exist. The most frequently used methods are those where the torque is calculated directly from the magnetic field solution in the motor. Such methods are the virtual work method, the magnetizing current method, and the Maxwell stress method (MSM). The accuracy of these methods depends to a great extent on the accuracy of the magnetic field calculation. In our case study we will use the MSM due to its simplicity.

In the MSM the torque is calculated on the basis of the magnetic field distribution on a closed surface in the air gap around the rotor [3,4]. The differential torque produced is:

$$d\mathbf{T} = \frac{1}{2} [(\mathbf{r} \times \underline{H})(\underline{n} \cdot \underline{B}) + (\mathbf{r} \times \underline{B})(\underline{n} \cdot \underline{H}) - (\mathbf{r} \times \underline{n})(\underline{H} \cdot \underline{B})] \quad (9)$$

The torque of the motor is obtained by creating a surface totally enclosing the rotor and integrating the

differential torque over that surface. Thus:

$$\mathbf{T} = \frac{1}{2} \oint ((\mathbf{r} \times \mathbf{H})(\mathbf{n} \cdot \mathbf{B}) + (\mathbf{r} \times \mathbf{B})(\mathbf{n} \cdot \mathbf{H}) - (\mathbf{r} \times \mathbf{n})(\mathbf{H} \cdot \mathbf{B})) dS \quad (10)$$

In the above equations \mathbf{r} is the position vector of the point of integration and \mathbf{n} denotes the unit vector normal to the surface. The torque is considered relative to the origin of the coordinate system located at the center of the stator.

BRUSHLESS DC MOTORS

A brushless DC motor consists of a rotor with permanent magnets and a stator with windings. Rotor motion is accomplished by generating a revolving magnetic field in the stator windings, which interacts with the permanent magnet fields. In fact, the magnets “chase” the rotating magnetic field and the energized winding of the stator switches just as the rotor aligns with the stator. The revolving field is created by sequentially energizing the winding phase pairs. The winding phase pairs are energized with current flow in a set sequence to produce the desired direction of rotation. At any instant, two of the three phases are energized while the third phase is off. This means that these motors do not operate directly off a DC voltage source. The actual excitation is either squarewave or sinewave current waveforms [5].

The most obvious advantage of the brushless configuration is that brush maintenance is no longer required and many problems associated with brushes do not exist. For example, brushes tend to produce radiofrequency interference and the sparking associated with them is a source of ignition in inflammable environments. In addition, brushless motors are potentially cleaner, faster, less noisy, and more reliable than induction motors. The rotor losses are very low and the stator is easily cooled because of the fine slot structure and the proximity of the outside air. Their main disadvantages are: (i) the need for shaft position sensing; and (ii) increased complexity in the electronic controller.

DEFINITION OF THE SAMPLE PROBLEM

Geometrical Characteristics

The geometrical characteristics of the brushless motors vary from type to type. Figure 1 illustrates

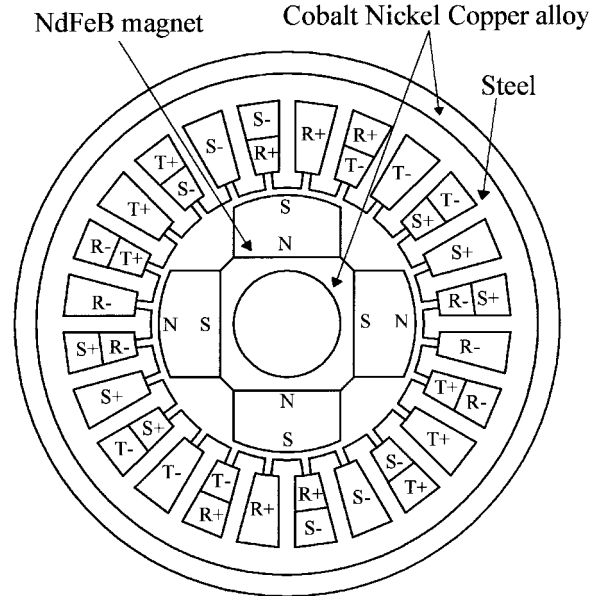


Figure 1 The two-dimensional cross section of the sample problem.

the two-dimensional cross section of the motor geometry which was selected as the sample problem to be analyzed. The stator is made of steel and has 24 slots and a three phase winding (denoted as R, S, and T). Any slot may contain conductors from one or two different phases. The rotor consists of a central non-magnetic shaft (modeled as air), surrounded by a Cobalt–Nickel–Copper alloy. Four uniformly magnetized Neodymium–Iron–Boron magnets are mounted on the rotor surface. The labels (N and S) inside each magnet show the location of its poles and hence the direction in which they are magnetized. The coils are loaded through a three-phase set-up, with each phase having into and out of plane directions. We use the labels: Coil R+, Coil R–, Coil S+, Coil S–, Coil T+, and Coil T–. The outer diameter of the motor is 72 mm and the axial length is 60 mm. It is assumed that magnetic flux losses to the outside are negligible and for this reason any air surrounding the motor will not be modeled.

Material Properties

Equation (8) denotes that we need to assign the values of the permeability for each material. For the nonlinear materials, such as the cobalt alloy and steel, the permeability as a function of the flux density is required. Manufacturers provide information about their material in the form of a B–H curve. From these curves we found the required functions by nonlinear

curve fitting. For the Cobalt–Nickel–Copper alloy we will use the equation:

$$\mu(B) = 8265 \cdot e^{\left(\frac{-(B-0.63)^{13}}{0.02}\right)} \cdot \left(1 - \frac{e^{\left(\frac{-B}{0.19}\right)}}{2.4}\right) + 295 \quad (11)$$

while for the steel the corresponding equation takes the form:

$$\mu(B) = \frac{5000}{1 - 0.05 \cdot B^2} + 200 \quad (12)$$

In the case of permanent magnets, manufacturers provide information in the form of a demagnetization curve, which lies in the second quadrant of the B – H plane. This curve indicates the remanent flux density B_r (for $H = 0$), the coercive field intensity H_c (for $B = 0$), and the manner in which B and H vary between these two points. Rare-earth materials, such as Neodymium–Iron–Boron (NdFeB) magnets, exhibit an almost linear demagnetization curve and as a result the linear model used in (4) is sufficient for properly modeling them. From a manufacturer of NdFeB magnets datasheet we read $B_r = 1.16$ T, $H_c = 883310$ A/m which according to:

$$B_r = \mu H_c \quad (13)$$

implies a relative permeability equal to 1.045.

PDEase IMPLEMENTATION

The Problem Descriptor File

In PDEase any problem to be solved is specified by means of a descriptor, which is simply a program written in the command language of the package. At first this seems rather cumbersome, but the advantage is that we can program our geometry using variables and then make changes very rapidly. A problem descriptor file is divided into sections. Each one describes a different type of information needed to specify the problem and is composed of statements.

The descriptor file for the brushless DC motor defined in the previous section is shown in Table 1, along with comments for each statement. It can be seen that each section begins with its pre-defined (reserved) name to inform PDEase of the nature of statements which it contains. PDEase processes a problem descriptor file from top to bottom and cannot

make forward references. For example variables can be used in the “Equations” section provided that they have been declared in a previous section. For this reason some parameters in the “Definitions” section of the descriptor file are reserved for later use. It must be pointed out that there is no need for user-input to define the triangular grid; the finite element mesh placement is automatic, although the user can alter the default settings of PDEase such as the grid density or the aspect ratio by adding the corresponding statements in the “Select” section [1]. The statement “stages = 2” is used to stabilize a nonlinear problem. In fact, this statement forces PDEase to run the descriptor file twice for different values for the relative permeabilities of cobalt alloy and steel. The first linear solution is used as an initial condition for the second non-linear one.

Importing a DXF Geometry File

In the “Boundaries” section of a descriptor file the user must specify the geometric model that defines the various regions or domains to be simulated. A model can be created either by using the “line” and/or “arc” statements of the command language of PDEase [1] or with the aid of a geometric modeler.

For complex geometries, like the motor presented in this paper, the use of a geometric modeler is most appropriate. Geometry data can be transferred from AutocadTM to PDEase using a Drawing Exchange File (DXF). However, in order to import a DXF file from Autocad to PDEase we must specially format the drawing. In general a drawing must be divided into regions, i.e., closed domains with definable material parameters that make up the physical geometry of the problem and all regions must be organized on layers [1]. As shown in Figure 2 the drawing of the motor consists of 15 layers. All drawing elements on a given layer are assigned the identical boundary conditions, which are specified as text on this layer.

RESULTS AND DISCUSSION

The finite element solution gives the potential at the nodes. This information by itself is usually of little interest in machinery analysis. We use this information to compute useful quantities such as flux density and torque. PDEase post-processing capabilities allow powerful generation and manipulation of graphics to provide a comprehensive understanding of any device.

Initially, the mesh resulting from the discretization process is shown in Figure 3. PDEase uses an adaptive mesh generation technique and the above

Table 1 Problem Descriptor File

Code Syntax	Comment
<i>Title</i> Brushless DC Motor	The Name of the Problem
<i>Select</i>	
stages = 2	We request two runs for the non-linear problem
errlim = 1e-5	Requested relative accuracy
ngrid = 50; aspect = 1.5	Parameters to control the mesh density
<i>Variables</i>	
A	Declare A to be the system variable.
<i>Definitions</i> {S.I. Units}	
mu0 = 4*pi*1.0e-7	Permeability of free space
mur1 = 1; mur2 = 1.045	Relative permeability of air and magnets respectively
J1 = 0	Current density in coils T+ and T-
J2 = 1500000	Current density in coils R+ and S-
J3 = -1500000	Current density in coils R- and S+
mur	Relative permeability parameter reserved
J	Current density parameter reserved
C = 883310	Coercive field intensity of NdFeB magnets
Hcx = 0; Hcy = 0	Coercive field intensity components
Hc = vector(Hcx,Hcy)	Coercive field intensity vector
H = curl(A)* (1/(mur*mu0))-Hc	Magnetic field intensity vector
Bxc = dy(A); Byc = -dx(A)	Magnetic flux density components
B = vector(Bxc,Byc)	Magnetic flux density vector
Babs = sqrt(Bxc**2+ Byc**2)	Magnitude of magnetic flux density
muralloy = if stage = 1 then 8265 else 8265*exp[-(Babs-0.63)**13/0.02]* [1-(exp(-Babs/0.19)/2.4)]+295	Relative permeability of Cobalt Alloy as a function of flux density (equation 11)
mursteel = if stage = 1 then 5000 else 5000/(1-0.05*(Babs)**2)+200	Relative permeability of steel as a function of flux density (equation 12)
Rho = vector(x,y)	The position vector of the (x,y) point
dTorque = 1/2*((cross(Rho,H)*(normal(B)))+ (cross(Rho,B))*(normal(H)))	Differential torque to be integrated along the air gap (equation 9)
<i>Equations</i>	
curl(H)-J = 0	The magnetostatic equation to be solved
<i>Boundaries</i>	
dxf_import(Motor = "motor.dxf")	Importation of the geometry file
feature 16	
start "circle" (-0.01745,0) arc(center = 0,0)	Draws a circle around the air gap
angle = -360	
<i>Plots</i>	
contour(A)	Contour plot of the magnetic vector potential A
surface(A)	Surface plot of A
vector(Bxc,Byc)	Vector plot of the flux density B
elevation(normal(B),tangential(B)) on "circle"	Bn and Bt along the air gap periphery
elevation(dTorque) on "circle"	The area under this plot equals the torque per unit of axial length of the motor
<i>End</i>	Declare the end of the descriptor file.

plot is the last and finer grid so that the field solution meets the accuracy requirements specified for this problem in the select section of the descriptor file. This final grid contains 10,369 nodes and 5,106 triangular elements. The meshing algorithm also detects the "feature" named "circle" and uses it to refine the mesh by adding extra nodes along the periphery of the

circle. This allows us to compute the fields in the air gap and the torque more accurately.

Figures 4 and 5 show a contour and surface plot respectively of the magnetic vector potential A over the whole model. From these figures it can be seen that the zero Dirichlet boundary condition that we imposed at the outer surface of the motor is identically

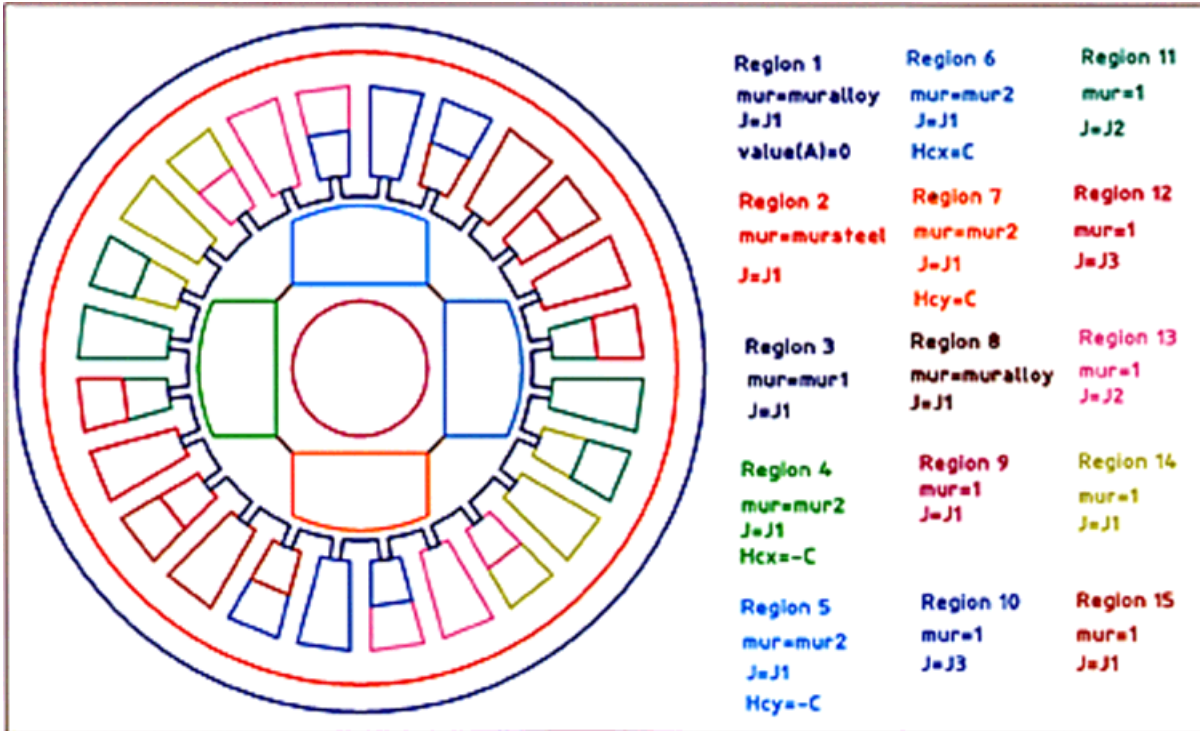


Figure 2 The imported geometry in DXF format.

satisfied. We can also observe the symmetry of the solution which reflects the symmetry of the geometry. The magnetic flux density strength and direction can be visualized through the use of a vector plot as shown in Figure 6. The vectors show the direction of the flux flow and their size show the magnitude. This figure indicates large flux density concentration in the air

gap between the stator and the rotor. It is well known that the air gap flux distribution is essential because the energy conversion is processed through the air gap. For this reason the normal and tangential components of the flux density along the air gap periphery are illustrated in Figure 7.

Finally, Figure 8 shows the differential torque along the air gap periphery. The area under this plot equals the torque per unit of axial length. To get the actual torque of the motor, this value has to be

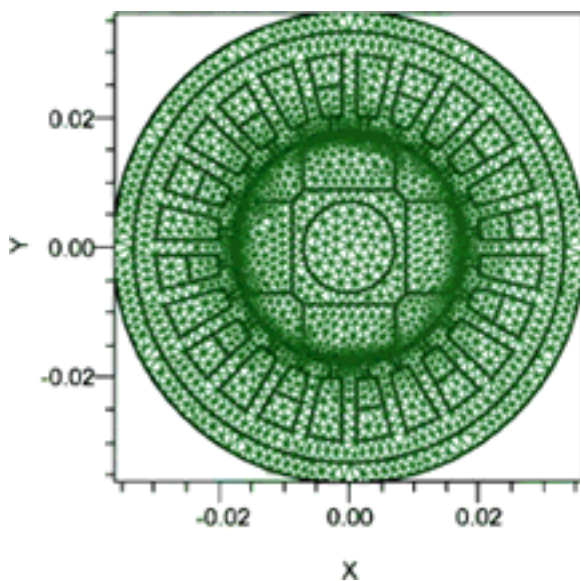


Figure 3 Discretization of the problem geometry.

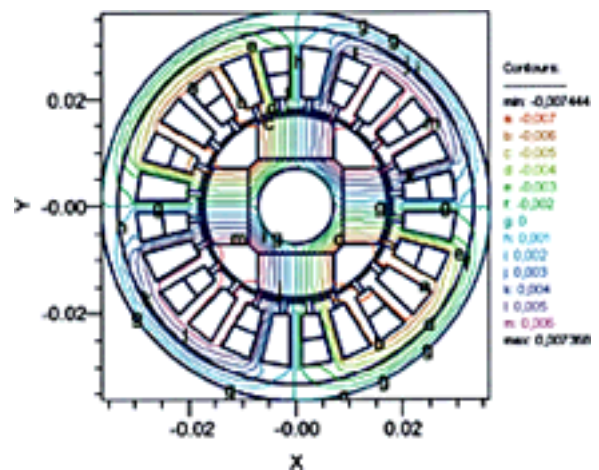


Figure 4 Contour lines of the magnetic potential A (Wb/m).

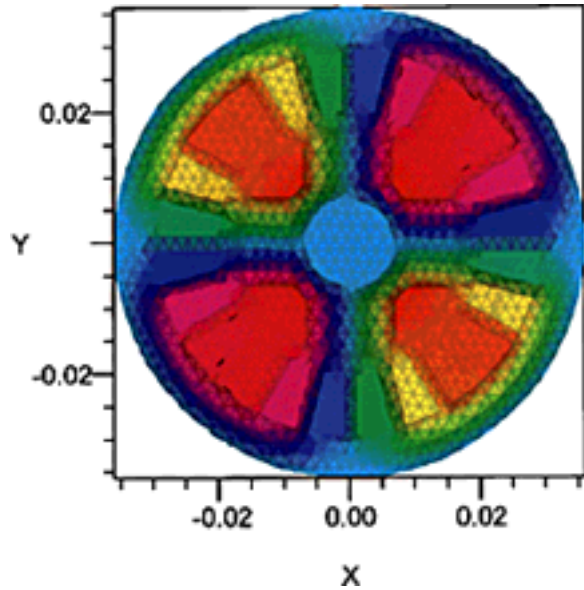


Figure 5 Surface plot of the magnetic potential A.

multiplied by its axial length. For the 60-mm long motor we have:

$$\begin{aligned} \text{Torque} &= 2.959 \text{ Nm/m} \times 60 \text{ mm} \\ &= 177.54 \times 10^{-3} \text{ Nm} \end{aligned} \quad (14)$$

To calculate the torque for different angular positions of the rotor we only have to rotate the rotor assembly (in the dxf file) and then re-execute the descriptor file. It is also possible to radially displace the rotor assembly with respect to the center of the stator, in order to study the effect of miscentering on the torque.

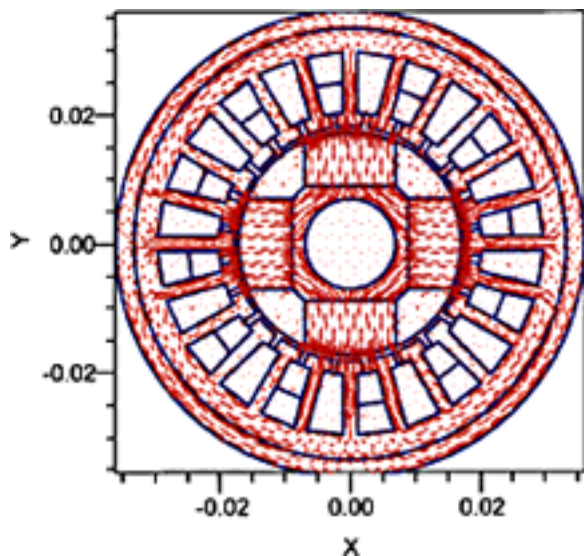


Figure 6 Vector plot of the flux density B.

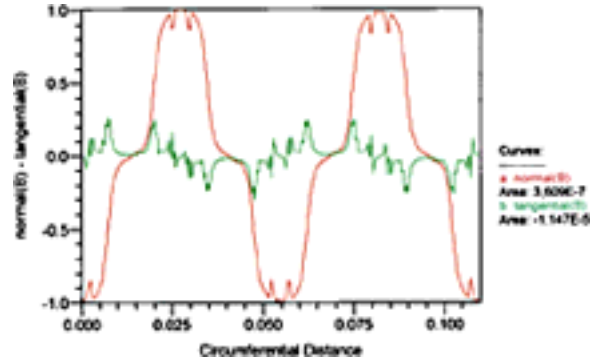


Figure 7 The normal and tangential components of the flux density along the air gap periphery.

In this case the third term in equation (9) must also be included in the corresponding statement of the descriptor file since $\underline{r} \times \underline{n}$ is no more zero.

A final remark concerns the fundamental question whether to perform a two- or three-dimensional analysis. Though a two-dimensional analysis may seem less accurate than a three-dimensional one, it actually may yield more accurate results when non-linear materials are present and the end effects are not important. Moreover, the time required for a two-dimensional simulation is often about 10% that of the three-dimensional one and thus the best approach is to perform the analysis and optimization in two-dimensional and then check the results in three-dimensional [6]. This validation could be done in FlexPDE™ [7], a three-dimensional partial differential equation solver, which uses virtually the same syntax as PDEase.

CONCLUSIONS

In this paper the application of the finite element method for the two dimensional magnetostatic analysis of a brushless DC motor was presented. The analysis was performed in the PDEase™ enviroment, a low

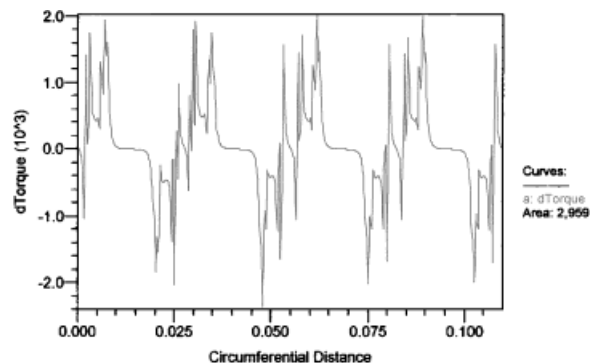
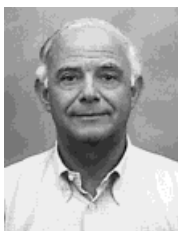


Figure 8 The differential torque along the air gap.

cost partial differential equation solver with automatic mesh generation and refinement capabilities. The descriptor file for this problem is remarkably short and easy to understand due to its very close to usual mathematical notation syntax. This kind of software can be very beneficial to engineering students in order to strengthen their understanding of field's theory differential form, boundary conditions, and the role of material properties. Additionally, it can raise student's interest and appreciation on abstract mathematical formulations because they can easily see their application and solution for real world problems. In this way they can acquire the solid background needed to use specialized packages.

BIOGRAPHIES



Vassilios Makios was born in Kavala, Greece. He received his electrical engineering degree (Dipl. Ing.) from the Technical University in Munich, Germany, in 1962 and the Ph.D (Dr. Ing.) from the Max Planck Institute for Plasmaphysics and the Technical University in Munich in 1966. From 1962 to 1967 he was Research Associate in the Max Planck Institute for Plasmaphysics in Munich, where he was associated with microwave interaction studies on plasmas. He served as Assistant Professor 1967–1970, Associate Professor 1970–1979, and Full Professor 1973–1977 in the Department of Electronics, Carleton University in Ottawa, Canada, where he was involved with teaching and research in microwave and optical communications, radar technology, remote sensing, and CO₂ laser development. From 1977, he is an Honorary Research Professor of Carleton University. From 1976, he is Professor of Engineering and Director of the Electromagnetics Laboratory in the Electrical Engineering Department of the University of Patras in Greece, where he is involved in teaching and research in microwave and optical communications, data communications networks, LAN's, MAN's, B-ISDN, and ATM technology with emphasis on efficient hardware implementations and rapid prototyping. His laboratory is actively participating in EU ACTS & ESPRIT R&D projects, e.g., LION, DISTIMA, PANORAMA, COBUCO etc. In 1986–1987, he spent his sabbatical year at the R&D laboratories of Siemens in Munich. He is also involved in research in photovoltaic systems. He has published over 130 papers and numerous patents in the above fields. He has participated in the organizing committees of numerous IEEE and European Conferences and was the Technical Program Chairman of the 5th Photovoltaic European Community Conference in Athens, 1983 and Co-Chairman of the EURINFO, 1988 Conference of the European Community. He is the recipient of the silver medal (1984) and the golden medal (1999) of the German Electrical Engineering Society (VDE). He is a senior member of the IEEE, member of the Canadian Association of Physicists, the German Physical Society, and the VDE, Professional Engineer of the Province

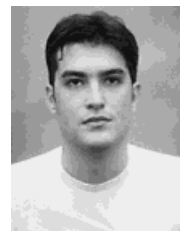
REFERENCES

- [1] PDEaseTM, Reference manual, tutorial, Handbook of demonstrations, Macsyma Inc, 1996.
- [2] N. Ida and J.P.A Bastos. Electromagnetics and calculation of fields, 2nd ed., Springer, New York, 1997, p.389.
- [3] A. F. L. Noqueira, "Limitations of the Conventional Methods of Force and Torque Prediction," Journal of ACES, 12(1)(1997), p. 74–79.
- [4] M. Trlep, A. Hamler, and B. Hribernik. "Various Approaches to Torque Calculations by FEM and BEM," Journal of ACES, 12(2)(1997), p. 127–130.
- [5] T. J. E. Miller, Brushless permanent-magnet and reluctance motor drives. Clarendon Press, Oxford, 1989, p. 55–58.
- [6] J. Sabonnadiere and A. Konrad, "Computing EM Fields," IEEE Spectrum, 29(11)(1992), p. 52–56.
- [7] FlexPDETM, PDE Solutions Inc.

of Ontario and the Greek Technical Chamber. He is currently Dean of Engineering from 1997 to-date and served also as Dean of Engineering in the period 1980–1982. For the past 12 years, he has served as the Vice President of the Research Committee of the University.



Constantinos Soras was born in Patras, Greece. He received both his electrical engineering diploma and Ph.D from the University of Patras, Greece in 1981 and 1989, respectively. From 1982 to 1989, he was Research Associate in the Electrical and Computer Engineering Department of the University of Patras, was involved with photovoltaic systems performance modeling. Since 1991, he has served as Lecturer in the Laboratory of Electromagnetics of the same department. He is teaching the basic electromagnetic courses and at the senior undergraduate/graduate level computational electromagnetics. His current research interests focus on computational electromagnetics, printed antennas, indoor radiowave propagation, and photovoltaic systems. He is member of the Technical Chamber of Greece, the International Solar Energy Society, and the Applied Computational Electromagnetics Society.



Antonios Kostaridis was born in Athens, Greece on 4 September 1976. He received his electrical engineering diploma from the University of Patras, Greece, in 1999. Currently he is a post-graduate student at the Laboratory of Electromagnetics, Department of Electrical and Computer Engineering of the University of Patras. His research interests include numerical solutions to electromagnetic radiation and scattering problems, printed antennas, and electromagnetic compatibility. He is a member of the Technical Chamber of Greece.